

CHAPTER 250

Backfilling Of Trenches Exposed to Waves

Jacob Hjelmager Jensen¹ and Jørgen Fredsøe²

Abstract

This paper treats the numerical prediction of initial and long-term morphology of small pipeline trenches. For this purpose a refined flow and sediment transport description is applied such that the entire mathematical problem is formulated and solved on a curvilinear grid using a $k - \epsilon$ turbulence-closure.

The backfilling process of trenches exposed to either waves or a steady current is of importance in relation to the implementation of pipelines in the marine environment. With respect to the sedimentation of trenches, the non-dimensional Trench-Keulegan-Carpenter number, $KC = a/L$, where a is the excursion length of a particle in waves and L the trench length, is investigated in detail, and an optimal KC -number for the backfilling rate is found. Coherent structures in the non-uniform unsteady trench-flow are shown to dominate the deposition rate when present.

The importance of a detailed description of the flow is further justified by comparing predictions of a very simple flow-model neglecting convective terms with the sophisticated flow-model.

Introduction

The morphodynamics of trenches or other man-made excavations in the marine environment involves the process of natural backfilling. In some cases backfilling is intended, as is the case with pipeline trenches, yet, in other cases, such as navigation channels, self-maintenance is striven for. For scientific as well as for economic reasons it is desirable to fully understand and control the mechanisms responsible for this specific morphological process.

A number of investigations of flow and sediment transport processes in a trench or a navigation channel have been conducted during the years. Bijker (1980), van Rijn (1986) and the analytical work of Fredsøe (1979) focus on the sediment transport processes. Other papers such as Alfrink's (1983) and Basara's (1995) focus on the sophisticated modelling of the hydrodynamics. These papers are all confined to the steady current case, and treat waves, if modelled, as a stirring mechanism for sediment only.

¹Ph.D.-student, ISVA, Tech. Univ. of Denmark, DK-2800 Lyngby, Denmark.

²Professor, ISVA, Tech. Univ. of Denmark, DK-2800 Lyngby, Denmark.

Deposition of sediment takes place whenever a suspended particle advected by the flow starts adapting to an environment with less capacity. This might happen when the velocity or the turbulent kinetic energy level of the fluid decreases. A change in fluid capacity is exactly what a particle travelling with the flow across a trench will experience. A net deposition of sediment within the boundaries of the trench may therefore take place. On top of that the bottom concentration of the suspended sediment decreases, which means that less sediment will erode from the bed. Another important contribution to the backfilling process is the action of gravity on bed-load particles moving on a sloping bed that makes particles go downhill more easily than uphill.

For particles carried by a steady stream past a trench the maximum change in capacity (depth-averaged velocity for instance) is obviously some function of the maximum expansion in depth. However, in the case of an oscillatory flow crossing the trench a suspended particle might not experience the maximum expansion in depth. For a given wave situation the expansion felt by a particle advected with the flow generally becomes a function of both the Trench-Keulegan-Carpenter-number and the maximum expansion in depth.

Problem

The trench is initially sinusoidal and characterized by a length, L , and a depth, h , see figure (1). The water depth is called D .

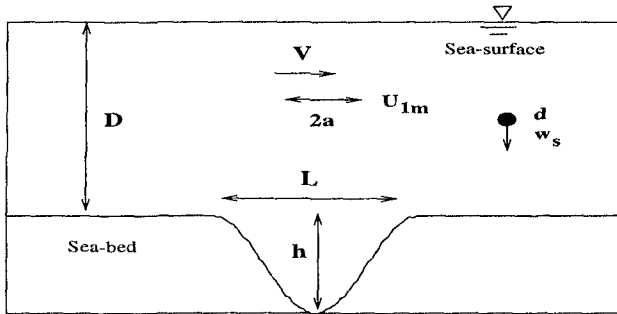


Figure 1: Sketch defining some of the key parameters used in the text.

The bed sediment is characterized by a fall velocity, w_s , and a diameter, d . The flow is generally combined by waves and currents (co-directional) and these are separately characterized by the fluxes, V and U_{1m} . The excursion length for a particle in a wave motion is symbolized by a . The wave is simulated by an oscillating pressure gradient neglecting any deformations of the water surface.

The initial backfilling rate is generally a function, Π , of all above-mentioned quantities, i.e.:

$$\Delta q = \Pi(L, h, D, d, w_s, a, V, U_{1m}, g)$$

where Δq is the amount of trapped sediment. A natural selection of non-dimensional

parameters from these quantities become:

$$\Delta\phi = \Psi\left(\frac{h}{L}, \frac{h}{D}, \theta, Z, KC, \frac{V}{V + U_{1m}}, \frac{k_N}{D}\right)$$

The parameters are in order of appearance referred to as: steepness, expansion, Shields, ($\theta = U_f^2/((s-1)gd)$) and Rouse parameter ($Z = U_f/(\kappa w_s)$), Trench-Keulegan-Carpenter number (a/L) and the wave/current parameter, where U_f is the friction velocity at a reference point far from the trench. The spatial coordinates, x (horizontal) and z (vertical), are non-dimensionalized by D and the time, t , by $(U_{1m} + V)/D$. For the present case the wave/current parameter is either 0 or 1, that is for waves and currents, respectively. All intermediate points define a combined wave/current flow. Furthermore, we will confine ourselves to an analysis based on the expansion parameter and the KC -number.

Solution of flow and sediment-transport equations

The finite volume concept (see Patankar (1980)) formulated in curvilinear orthogonal multi-block coordinates is applied, solving the transformed continuity equation and the fully 2D transformed Reynolds-averaged Navier-Stokes equations employing the standard $k - \epsilon$ closure of turbulence. A thorough description of the present model is reported by Tjerry (1997).

The partial differential equations of the turbulence model in Cartesian form, i.e. turbulent kinetic energy, k , and dissipation of turbulent kinetic energy, ϵ , are given by:

$$\frac{\partial k}{\partial t} + \frac{\partial u_j k}{\partial x_j} - \frac{\partial}{\partial x_j} \left(\frac{\nu_T}{\sigma_k} \frac{\partial k}{\partial x_j} \right) = \nu_T \frac{\partial u_i}{\partial x_j} \left(\frac{\partial u_j}{\partial x_j} + \frac{\partial u_j}{\partial x_i} \right) - \epsilon \quad (1)$$

$$\frac{\partial \epsilon}{\partial t} + \frac{\partial u_j \epsilon}{\partial x_j} - \frac{\partial}{\partial x_j} \left(\frac{\nu_T}{\sigma_\epsilon} \frac{\partial \epsilon}{\partial x_j} \right) = C_{\epsilon 1} \frac{\epsilon}{k} \nu_T \frac{\partial u_i}{\partial x_j} \left(\frac{\partial u_j}{\partial x_j} + \frac{\partial u_j}{\partial x_i} \right) - C_{\epsilon 2} \frac{\epsilon^2}{k} \quad (2)$$

Here, t is time, x_i the spatial coordinates, u_i the velocities and ν_T is the eddy-viscosity, calculated from:

$$\nu_T = C_\mu \frac{k^2}{\epsilon} \quad (3)$$

The set of constants that appears in the $k - \epsilon$ model is standard choice and originally proposed by Launder (1974):

C_μ	σ_k	σ_ϵ	$C_{\epsilon 1}$	$C_{\epsilon 2}$
0.09	1.0	1.3	1.44	1.92

The transport of sediment, q , is divided into a bed and a suspended load contribution and corrected with the porosity, n , implicitly. The non-dimensional bed load, ϕ_B , is calculated using the Meyer-Peter formula modifying tractive stresses with slope effects as suggested by Fredsøe (1978):

$$\phi_B = \frac{q_B/(1-n)}{\sqrt{(s-1)gd^3}} = \frac{8}{(1-n)} (\theta - \theta_c - 0.1 \frac{\partial h}{\partial x})^{3/2} \quad (4)$$

where q_B is the bed load, $\partial h/\partial x$ the slope of the bed, g the acceleration of gravity, s the relative density and θ_c the critical Shields parameter (~ 0.05).

The concentration of suspended sediment is derived by solving the transport equation:

$$\frac{\partial c}{\partial t} + u \frac{\partial c}{\partial x} + v \frac{\partial c}{\partial z} = w_s \frac{\partial c}{\partial z} + \frac{\partial}{\partial x}(\nu_T \frac{\partial c}{\partial x}) + \frac{\partial}{\partial z}(\nu_T \frac{\partial c}{\partial z}) \quad (5)$$

The non-dimensional suspended transport, ϕ_S , is found as:

$$\phi_S = \frac{q_S/(1-n)}{\sqrt{(s-1)gd^3}} = \frac{\int_{-h}^1 cudz/(1-n)}{\sqrt{(s-1)gd^3}} \quad (6)$$

where q_S is the suspended transport, and u and v are the longitudinal and vertical velocities, respectively.

Intra-wave calculation is applied for the sediment-transport model in order to take into account non-linear and phase-lag effects.

In the present model the water surface is taken to be plane, and the waves are introduced as an oscillatory motion caused by an oscillatory pressure gradient. At the water surface the flow equations apply symmetry conditions while the c -equation applies a no-flux condition. At the bed boundary a no-slip condition is used for the momentum equations, and a Dirichlet condition is used for the c -equation as the Engelund-Fredsoe formula (1976) is applied, i.e. $c_b = c_b(\theta)$, where c_b is the concentration at bed level.

Furthermore the k -equation uses a no-flux condition at the bed, and the bed condition for the ϵ -equation reads: $\epsilon = (30C_\mu^{0.75})/(\kappa k_N/D)k^3/2$, where k_N/D is the relative roughness of the sea-bed and κ the von Karman mixing length constant. On the in- and outlets Dirichlet and Neumann are applied, respectively, if not, periodic conditions are used.

The total flux of sediment is used in a continuity equation, which governs the morphodynamics. This reads:

$$\frac{\partial h}{\partial t} + \frac{\partial q}{\partial x} = 0 \quad (7)$$

stating that the divergence of depth-integrated sediment flux, $q = q_B + q_S$, is equal to the rate of change in bed elevation, h . This equation is discretized with a second order accurate scheme minimizing numerical diffusion. This is crucial when predicting diffusive processes such as backfilling of trenches.

If the entire flow, sediment, and morphological modules are run together, the dynamics of a mobile bed can be described and the backfilling tracked.

Backfilling in currents

In addition to the $k - \epsilon$ model an alternative flow description of the depth-averaged type is employed for the steady state case to emphasize the effect of including a more refined flow description. The depth-averaged approach uses a prescribed logarithmic velocity profile matched by the flux of water and a parabolic eddy-viscosity distribution

scaled with the friction velocity. This is identical to a flow solution where convective terms have been ignored, i.e. local equilibrium.

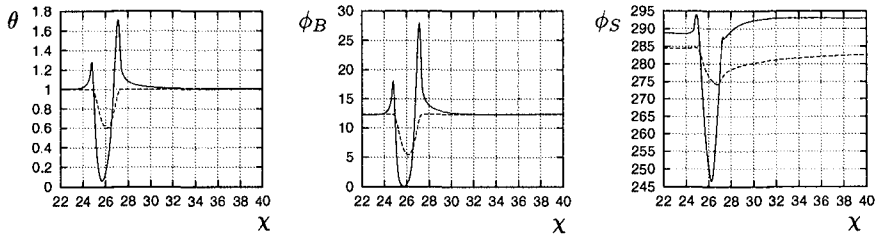


Figure 2: The Shields parameter along with the non-dimensional bed and suspended load distributions across a trench with the deepest section of the trench at $x = 26$ predicted by a $k - \epsilon$ model and a depth-averaged model. Reference flow: \rightarrow . Parameters are: $L/h=10$, $\theta=1$, $h/D = 0.25$ and $Z=0.6$. $k - \epsilon$ model: —, Depth-averaged model: - - -.

The depth-averaged approach has earlier been applied in the field of sediment transport for analytical purposes, and it is therefore of interest to compare the performance of these flow models with respect to morphology (cf. e.g. Fredsøe (1979)).

The shear stress along with the non-dimensional bed and suspended load predicted by the two flow models typically vary as illustrated in figure (2). It is obvious from the shear-stress variation (i.e. $\theta(x)$) that the depth-averaged approach cannot in detail capture the complex behaviour of flow over a negative bump, which involves separation (or retardation), a phase shift between shear stress and bed form, speed-up and the relaxation of speed-up.

It is seen from figure (2) that both models predict erosion and deposition on the down- and upstream trench side, respectively. The additional shear stress features uncovered by the $k - \epsilon$ model relate in a morphological sense to a faster migration, a slower backfill (partly due to the above mentioned phase shift) and a more violent downstream deformation. The progressing asymmetrical shape of the bed, $h(x)$, is captured with both models as seen in figure (3), where bed forms at $T = tV/D=3000$, 9000, 18000 and 28000 are shown.

It is surprising how well the depth-averaged flow model performs in general and with respect to backfilling in particular. One reason for this is that the sediment transport mechanics such as the response length of suspended sediment is the governing parameter for the backfilling, and that very detailed flow mechanics to some extent is unnecessary. However, for $h/D \rightarrow 0$ (deep-water case) the depth-averaged model must fail since the gradient in capacity as well as in bottom concentration approaches zero in the limit. In this case the depth-averaged mechanism is not capable of explaining the deposition process, and a detailed description of the flow past a trench, including separation or even flow retardation, becomes necessary.

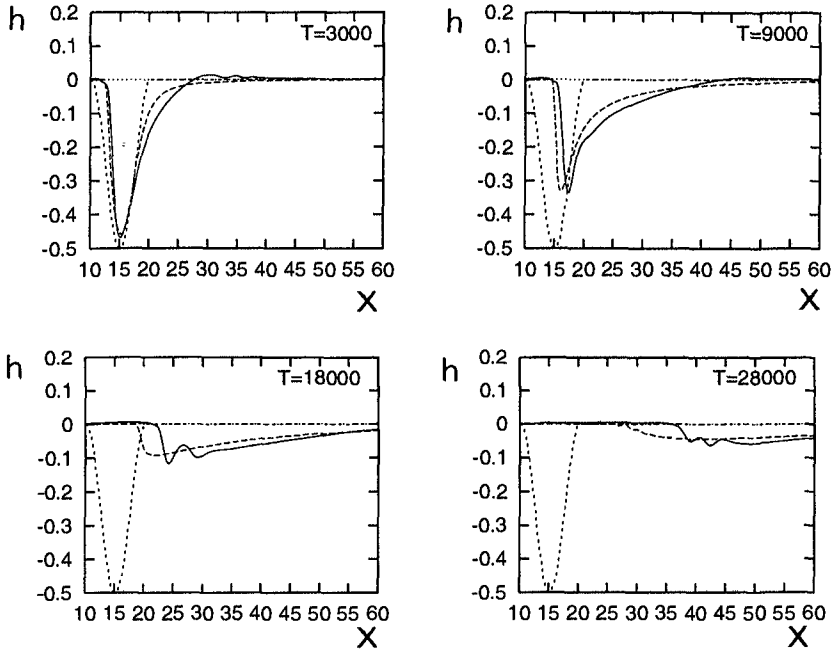


Figure 3: Shape of trench at four stages of its morphological evolution, for $k_N/D = 0.001$, $w_s/V = 0.02$ and $\theta = 0.25$. Reference flow (current alone): \rightarrow . $k - \epsilon$ model: —, Depth-averaged model: - - -, Initial trench shape: - - - -.

Backfilling in waves

If wave effects are included matters become more complicated. The waves introduce an additional parameter that in non-dimensional form is described by a KC -number. This is the Keulegan-Carpenter number well-known from the offshore hydrodynamics where it is defined as:

$$KC = \frac{2\pi a}{D_c}$$

in which D_c = the diameter of the cylinder. For small KC -numbers ($< 1-2$) flow separation will not occur, while at larger KC -numbers ($> 10-20$), the flow is fully separated. In trenches, the flow may also separate if the slope is steep enough, and the equivalent KC -number is sufficiently large. In the following we define this number by:

$$KC = a/L$$

With respect to the sedimentation of trenches the KC -number involves at least one important aspect other than flow-separation. For $KC \sim 1$ it is seen that a sand particle picked up on the plane bed may reach the deepest part of the trench where it may settle due to a reduced capacity. The capacity is reduced on the upstream slope as the depth increases (non-uniformity) and as the flow decelerates (unsteadiness), which

gives rise to smaller flow velocities as well as a decrease in intensity of turbulent kinetic energy.

So this is what happens: As suspended particles adapt to the local flow capacity by settling, they might get trapped in the separation bubble growing simultaneously on the upstream slope. If the vortex (former separation bubble) maintains its rotation and is able to keep the particles 'alive' when ejected at flow reversal, particles will be convected out of the trench and into the outer flow with the vortex.

The situation described is captured in figure (4) where time series of contours of concentration and turbulent kinetic energy are shown side by side for a short span of time around flow reversal. The phase in the wave period is symbolized as a dot on the sine-curve (positive values indicate left- to right-going flow).

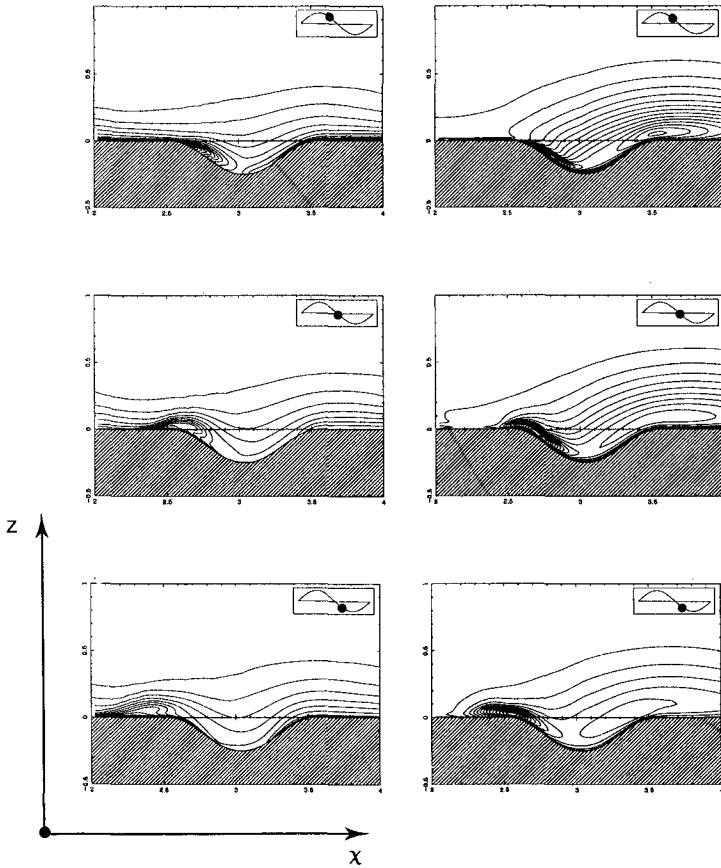


Figure 4: Time series of contours of concentration (left hand side of figure) and turbulent kinetic energy (right hand side of figure) around flow reversal. For $L/h=5$, $\theta=1$, $h/D=0.25$, $w_s/U_{1m}=0.02$ and $KC=1$.

While the separation develops on the upstream slope, the speed-up of fluid on the downstream trench-shoulder creates high shear-stress levels, which causes a large amount of sediment to suspend. This is seen in figure (5) where time series of profiles for horizontal velocities and contours of concentration are placed side by side at a phase close to flow reversal. The speed-up process in the converging section is visualised by sediment being bursted off the sloping trench bed. This results in an overloaded cloud of sediment that returns with the reversing flow to deeper parts of the trench where it most likely will be deposited. This process, captured in figure (5), may intensify the backfilling.

The time series of concentration contours shown in figure (5) are created by shutting off the bed erosion shortly before the reversal of the flow occurs.

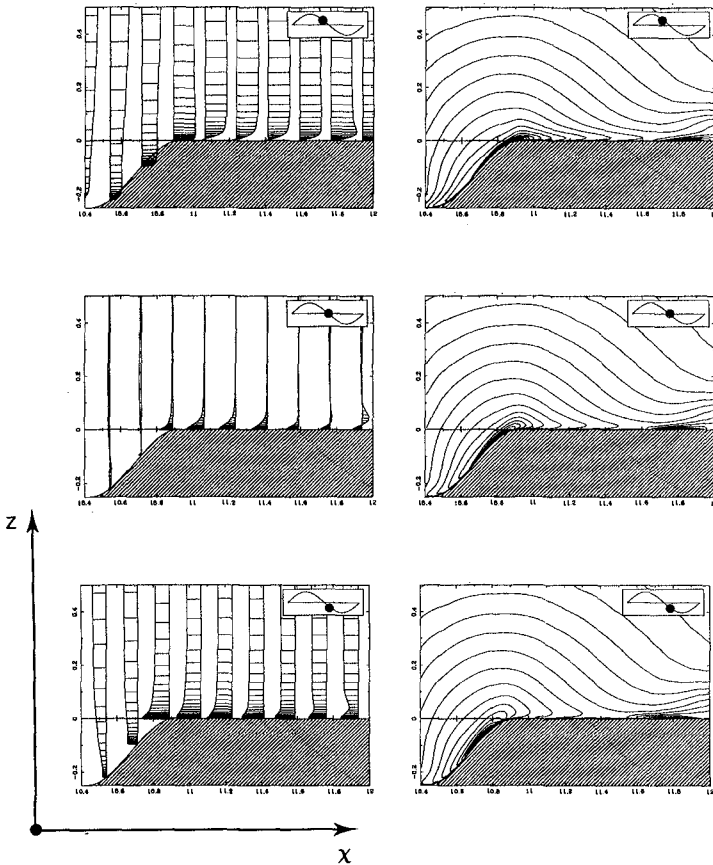


Figure 5: Time series of profiles of horizontal velocities (left hand side of figure) and contours of concentration (right hand side of figure). For $L/h=5$, $\theta=1$, $h/D=0.25$, $w_s/U_{1m}=0.02$ and $KC=1$.

The non-uniform and unsteady flow separates and will speed-up succeedingly, which in the period-averaged sense will create a near bed flow directed towards the banks. A return flow, required for reasons of continuity, is therefore directed towards the centre of the trench so that the time-averaged streamline pattern, depicted in figure (6), shows two cells rotating clock- and anti-clockwise on the left and right hand side, respectively. It is also worth noticing that two additional rotating cells will develop on the shoulders of the trench.

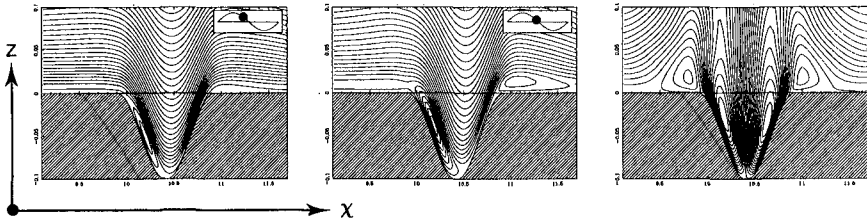


Figure 6: Two patterns of instant streamlines just before flow reversal occurs (in both cases the direction of main flow: \rightarrow) along with the corresponding period-averaged streamline pattern. $KC=0.5$, $h/D=0.1$, $L/h=10$, $k_N/D=0.001$.

The result seen on the right hand side of figure (6) is a time-integrated effect from using a detailed flow-description.

Distributions of the time-averaged bed and suspended loads are shown in figure (7). With the streaming pattern in mind it is interesting to study the period-averaged bed load distribution in the neighbourhood of the trench. The resulting transport rate is an outcome of a battle between the action of gravity and the time-averaged shear stress. It is seen that the gradient, $\partial q_B/\partial x$, which determines whether the sinusoidal trench is being eroded (positive) or sediment is being deposited (negative) in some cases may shift sign at the centre of the trench, such that the deepest regions of the trench is eroded. The cases where the deepest regions are eroded are, for this particular span of parameters, found (see left hand side of figure (7)) as the KC -number is increased and the steepness parameter decreased, thus the time-averaged hydrodynamical forces are strengthened and the gravitational forces weakened.

The period-averaged rotating cells which appear on top of the shoulders are reflected in the bed transport, $\bar{\phi}_B$, at that particular location. This is shown on the left hand side of figure (7). The bed transport here are, however, damped by the vortices (increases in strength with the KC -number) which pass through the shoulder region shortly after flow reversal.

The influence of the vortex on $\bar{\phi}_B$ and $\bar{\phi}_S$ at a given location on the flat bed is recognized as a departure from $\bar{\phi}_B = 0$ and $\bar{\phi}_S = 0$. The vortex disturbs the flat bed region at a distance which is of the same order as the excursion length and is for obvious reasons amplified as h/L is increased. On the flat bed the sediment transport is, in the time-averaged sense, directed away from the trench by the strength of the advected vortex.

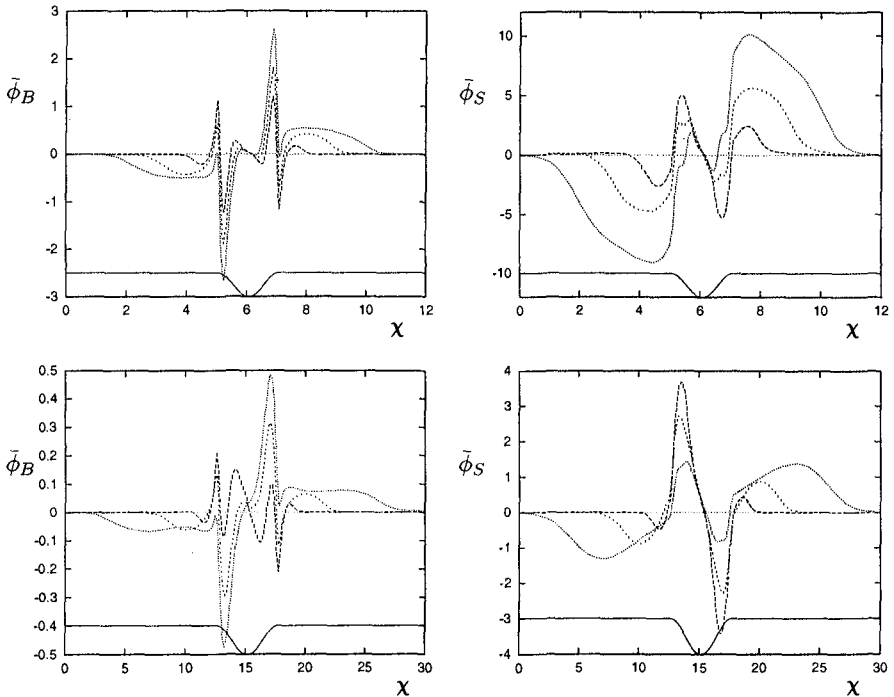


Figure 7: Distribution of period-averaged bed (left-hand side) and suspended sediment transport (right hand side) for a steep ($L/h = 4$ for the top of figure) and a moderate trench slope ($L/h = 10$ for the bottom of figure). $KC = 1.0$: $\cdots\cdots$, $KC = 0.5$: $-\ - -$, $KC = 0.25$: $-\ \cdot - \cdot$, with $h/D = 0.5$, $\theta = 0.65$ and $w_s/U_{1m} = 0.02$. The trench height depicted is highly distorted.

At the deeper regions of the trench the suspended sediment transport, $\bar{\phi}_S$, is directed towards the centre (see right hand side of figure (7)), implying that suspended material will be deposited here as opposed to erosion of the shoulder region.

More generally the backfilling process can be analysed by looking at period-averaged trapped sediment within control boxes (CB). Figure (8) shows the amount of trapped sediment as a function of the KC -number for three expansion parameters in two control boxes; an inner and an outer. The outer control box surrounds the entire trench from shoulder to shoulder, and the inner control box is bounded by the two steepest sections of the trench.

The trapped sediment is furthermore divided into contributions from bed and suspended load and where deposition is assigned with positive values. The Shields parameter in these calculations are: $\theta = 1$, and the steepness: $h/L = 0.1$.

An interesting feature of figure (8) is that an optimal backfilling rate takes place at $KC \sim 0.2$ for the suspended sediment. This is before the vortex mechanism becomes dominant. At this point the backfilling rate drops as the separation bubble grows in size

and strength. However, beyond a certain KC -number the strength of the separation bubble will not increase any more, which is evident in figure (8) where a small increase in deposition of suspended sediment is seen for large KC -numbers.

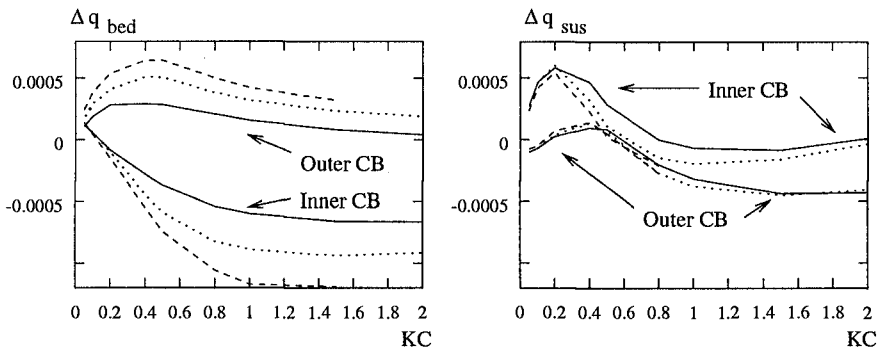


Figure 8: Trapped bed, (left hand side) and suspended load (right hand side) within control boxes (CB) for $h/D = 0.05$: - - -, $h/D = 0.10$: ····· and $h/D = 0.25$: ———, and $L/h = 10$, $\theta = 1$, $Z = 0.6$.

The trapped sediment originating from bed load is of the same order of magnitude but negative as the trapped suspended load (at least when $\theta = 1$ and $L/h = 10$) even though $q_{S,max} \gg q_{B,max}$. It is seen from the left hand side of figure (8) (inner CB) that the action of gravity for this particular steepness parameter is merely capable of reducing the forces from the time-averaged shear-stress.

The time-averaged rotating cells on the shoulders are also seen to affect the in-fill of bed load through the outer box. This in-fill rate decreases as the KC -number increases because the separation bubble is washed over the shoulder thus counteracting this time-averaged motion.

It is clear from figure (8) that the typical morphological evolution is a net erosion of the trench shoulders together with a deposition in the centre of the trench. This is, however, exactly the way a diffusion process works.

The morphological development of a trench exposed to waves has been calculated using both flow models discussed previously. Four selected results are shown in figure (9), which clearly demonstrates the diffusion-like process.

As opposed to the steady current case, the depth-averaged model performs poorly in the pure wave case. This is not surprising since a detailed flow description is required to resolve the significant effect from the separation bubble dynamics on the backfilling process in waves. This causes the depth-averaged model to predict a faster backfill.

One interesting, but not surprising, consequence of the change in bed shape was the slow vanishing of the separation bubble as the trench slope becomes gentler. This involves a similar decrease in the vortex mechanism. One would immediately guess that this would lead to an increase in the backfilling rate. However, the trench widens and with this a decrease in the effective KC -number was found. After $T = tU_{1m}/D = 1000$ the change in bed form was extremely weak.

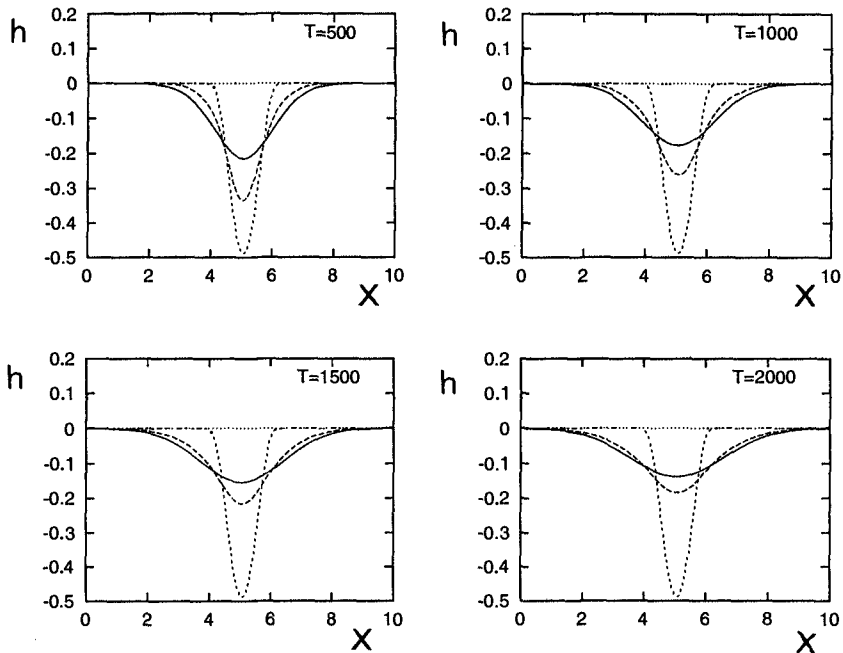


Figure 9: Shape of trench at four stages of its morphological evolution, for $k_N/D = 0.001$, $w_s/U_{1m} = 0.02$, $\theta = 0.25$ and $KC = 0.2$. $k - \epsilon$ model: - - -, Depth-averaged model: —, Initial trench shape: - - - -.

Conclusion

The dynamics of vortices originally born as separation bubbles seem to dominate the backfilling process in waves whenever they are present. This is because the separation bubble traps incoming sediment particles on the upstream slope and keeps some of these 'alive' by the massive level of turbulent kinetic energy found in separating regions. When it detaches from the surface at flow reversal, a cloud of sediment will be advected out of the trench with the vortex.

It has been shown that the vortex mechanism is important and that models which neglect this process may over-predict the backfilling rate.

The optimal backfilling rate in waves was found to be $KC \sim 0.2$.

Furthermore, depth-averaged steady state flow models give good results when applied in morphological calculations particularly in shallow waters which include navigation channels etc.. However, these simple flow models fail to describe more complicated KC -effects found in waves as the effect of separation and vortex shedding is not taken into account.

Acknowledgments.

The computer-code applied in the present investigation is originally developed at ISVA by Ph.D. Søren Tjerry.

This work is jointly supported by "Numerical and Experimental Fluid Mechanics" and "Marine Technique" both funded by the Danish Technical Research Council (STVF).

References

- Alfrink, B.J., and van Rijn, L.C. (1983). Two-equation turbulence model for flow over trenches. *Journal of Hydraulic Engineering (ASCE)*, Vol. 109, No.7, pp. 941-958.
- Basara, B. and Younis B.A. (1995). Prediction of turbulent flows in dredged trenches. *Journal of Hydraulic Research*, Vol. 33, No. 6.
- Bijker, E.W. (1980). Sedimentation in channels and trenches. Proc., 17'th ICCE'80, Vol 2. pp. 1708-1718, Sydney, Australia.
- Engelund, F. and Fredsøe J. (1976). A sediment transport model for straight alluvial channels. *Nordic Hydrology* 7:293-306.
- Fredsøe, J. (1978). Sedimentation of river navigation channels. *Journal of the Hydraulics Division (ASCE)*, Vol. 104, No. HY2, pp.223-236.
- Fredsøe, J. (1979). Natural backfilling of pipeline trenches. *Journal of Petroleum Techn. Vol. 31*, pp. 1223-1230.
- Lauder, B.E. and Spalding, D.B. (1974). The numerical computation of turbulent flows. *Comput. Meths. Appl. Mech. Eng.*, 3:269-289.
- Patankar, S.V. (1980). *Numerical Heat Transfer and Fluid Flows*. Hemisphere, New York.
- Tjerry, S. (1997). *Morphological Calculations of Dunes in Alluvial Rivers*. Ph.D.-thesis ISVA, Technical University of Denmark. (In print).
- van Rijn, L.C. (1986). *Sedimentation of Dredged Channels by Currents and Waves*. Delft Hydraulics Laboratory. Delft Hydraulics Communication No. 369.